Research Article

Thickness Effect on F8T2/C$_{60}$ Bilayer Photovoltaic Devices

Natasha A. D. Yamamoto, Andreia G. Macedo, and Lucimara S. Roman

Grupo de Dispositivos Nanoestruturados, Departamento de Física, Universidade Federal do Paraná, 8153-990 Curitiba, PR, Brazil

Correspondence should be addressed to Lucimara S. Roman, lsroman@fisica.ufpr.br

Copolymers based on fluorene-thiophene units have presented promising efficiencies in photovoltaic devices applications. They present good transport properties mainly after thermal treatment of the polymer films. Here, we investigate the properties of bilayer devices formed by the heterojunction of the polymer F8T2 with variable thickness and the fullerene. The series resistance of the equivalent circuit associated with the device increases as the polymer film gets thicker. The current-voltage characteristics of the bilayer devices follow the Mott-Gurney law of SCLC. For the best performing device we measured 2.1% of power conversion efficiency.

1. Introduction

Fluorene-thiophene-conjugated copolymers have been extensively investigated and used in the field of organic electronics [1, 2]. The main applications are organic photovoltaic cells (PVs) [3–10], organic light-emitting diodes (OLEDs) [11], and field effect transistors (FETs) [12]. These copolymers have high absorption coefficient in the visible wavelength range; high quantum yields values and high charge mobility. Additionally, the incorporation of carbon-based materials, such as carbon nanotubes [9], fullerenes or its derivatives [13–15] brought interesting effects in organic PV cells built in bulk heterojunction (BHJ) or layered geometry. These carbon compounds have high electron affinity relatively to the conjugated polymers; in this way, they act as electron acceptor materials favoring the exciton dissociation prior the radiative/nonradiative recombinations, thus the charge collection through the electrodes.

This combination has resulted in high power conversion efficiencies (η). For instance, BHJ cell based on poly (9,9'-dihexylfluorene-alt-thiophene) polymer (PFT1) and PCBM displayed open circuit voltage (V_{oc}) of 0.77 V and η of 0.62% [3], while using poly(9,9'-dihexylfluorene-alt-bithiophene) (F6T2) or poly[9,9'-dioctyl-fluorene-cobithiophene] (F8T2) displayed V_{oc} around 1 V, η of 2.7% [4] or

2.13% [5, 6], respectively. These results were both attributed to the high hole mobility and absorption coefficient in these polymers with efficient photocurrent generation. A bilayer solar cell prepared with F8T2 but different fullerene C$_{70}$ displayed the highest η of 3.4%, after thermal annealing at 200°C [7]. The increase in η in this device was attributed to a better chain organization and higher roughness of the film, achieving higher donor-acceptor heterojunction area for exciton dissociation. Recently, we reported a bilayer PV cell prepared with poly [9,9'-hexyl-fluorene-alt-bithiophene] and fullerene (C$_{60}$) displaying an increase of η from 0.4 to 2.8% after annealing at 200°C. Comparing these results and the behavior of the current versus voltage characteristics, we concluded that the π-π stacking in solid state is enhanced after thermal annealing with a reduction of traps and thus reflecting higher hole mobility in this polymer after annealing [8].

Herein, we report the studies of bilayer devices formed by the heterojunction of the polymer F8T2 with variable thickness (18 up to 60 nm) and the fullerene C$_{60}$ sandwiched between two electrodes: FTO/PEDOT : PSS as the anode and aluminium as the cathode. The transport properties of the devices follow the Mott-Gurney law of space charge law current (SCLC).
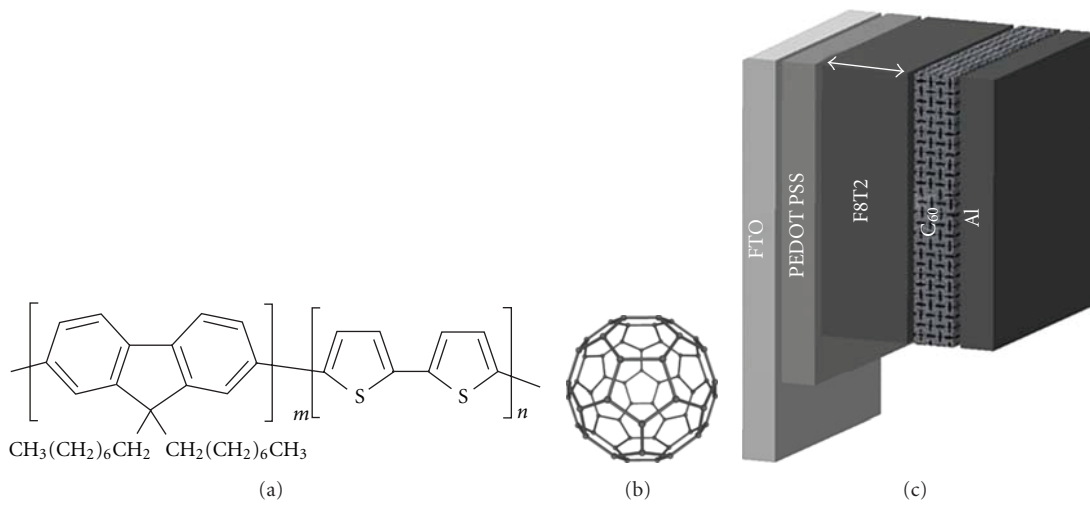
FIGURE 1: Molecular structures of the active materials: (a) structure of F8T2 polymer, (b) fullerene C_{60}, and (c) bilayer device structure: FTO/PEDOT : PSS/F8T2/C_{60}/Al with variable thickness of the F8T2 layer.
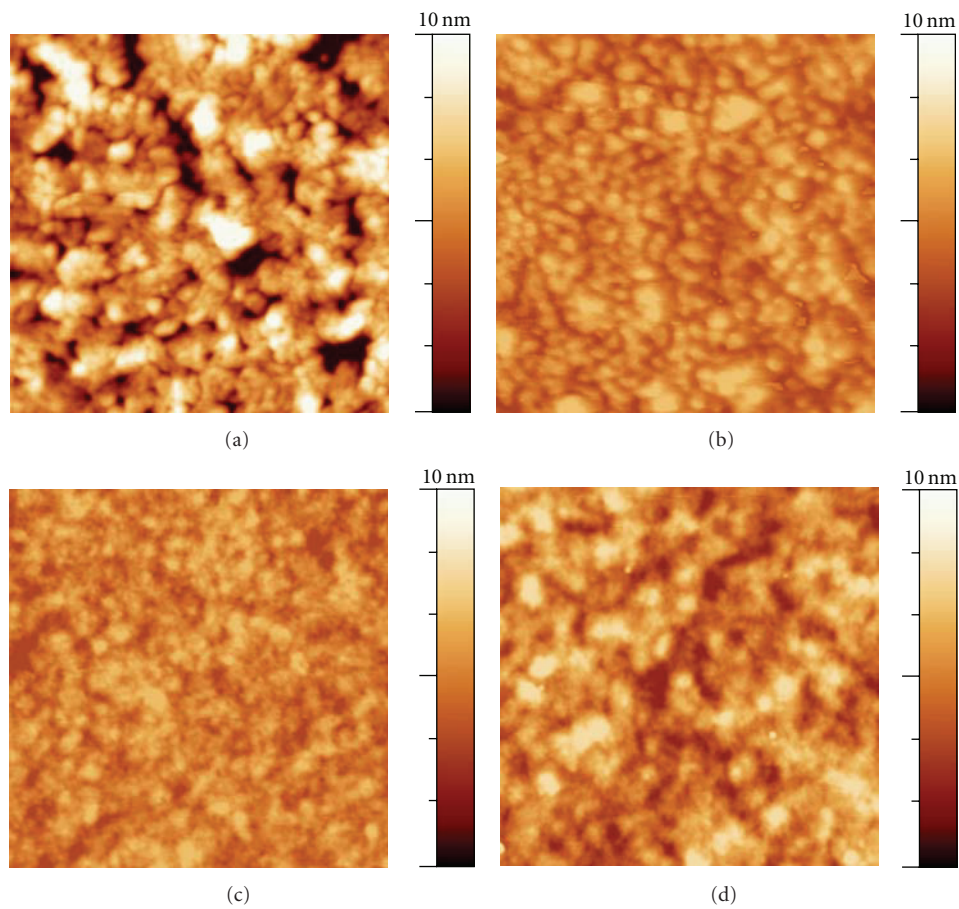

FIGURE 2: AFM height images of F8T2 polymer films coated on glass substrates for each thickness: (a) 18 nm, (b) 30 nm, (c) 40 nm, and (d) 60 nm. The scan size is $1.5\,\mu$m $\times$ $1.5\,\mu$m.
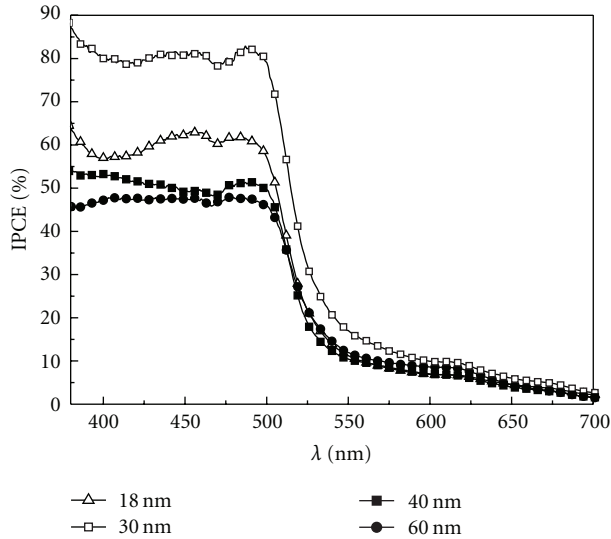
Figure 3: External quantum efficiency for the FTO/PEDOT:PSS/F8T2/C$_{60}$/Al devices with different thickness of the F8T2 layer.

Table 1: Device characteristics of the bilayer solar cells.

Active layer thickness (nm)	J_{sc} (mA cm^{-2})	V_{oc} (V)	FF (%)	η (%)
18	3.84	0.75	54	1.60
30	4.79	0.91	50	2.10
40	3.65	0.85	50	1.55
60	1.97	0.65	34	0.43

2. Experimental

Poly(9,9-dioctylfluorene-*alt*-bithiophene) (F8T2) polymer with number average molecular weight (M$_n$) >20,000 gmol^{-1} was purchased from Aldrich. The devices were fabricated as follows: poly(3,4-ethylenedioxythiophene)-polystyrene sulfonic acid (PEDOT:PSS) was filtered in a 0.45 μm filter, then a film with thickness of 40 nm was spin coated at 6000 rpm onto the cleaned fluorine-tin-oxide (FTO-, 5–10 Ω) [16] patterned glass substrate and annealed at 100°C by 15 min in air. F8T2 polymer film was spin coated from chlorobenzene solutions with concentrations of 3–7.5 mgmL^{-1} and treated at 100°C by 15 min (in vacuum). These parameters were set in order to obtain active layer thickness ranging from 18 to 60 nm. Then, 30 nm of C$_{60}$ and 100 nm of Al were thermally evaporated through a shadow mask at vacuum pressure of 6×10^{-6} mbar, respectively. Subsequently, the FTO/PEDOT:PSS/F8T2/C$_{60}$/Al were encapsulated upon nitrogen atmosphere. The F8T2 and C$_{60}$ molecular structures as well as the device structure are depicted in Figure 1.

The polymer films thickness was determined in a Dektak 3 profilometer. Topography images were acquired by using an atomic force microscope (AFM, Shimadzu SPM 9500J3) in dynamic mode. The photovoltaic characterization was performed with a Keithley picoammeter with power supply, model 6487 and a monochromator/spectrometer (1/4 m Oriel). The solar simulation was made using air mass (AM1.5) filter with a power illumination of 100 mWcm^{-2} from a 150 W Oriel Xenon lamp.

3. Results and Discussion

F8T2 films were analyzed by AFM as illustrated in Figures 2(a)–2(d). Similar morphology is observed by varying the thickness from 18 up to 60 nm, however the film with 18 nm has root-mean-square (rms) roughness equal to 1.2 nm, and this value is slightly higher in comparison with thicker films

that display roughness below 1 nm. This may arise due to the roughness related with the FTO substrate; PEDOT:PSS and thicker polymer films cover more efficiently the valleys and hills observed in polycrystalline FTO films.

The photovoltaic devices were characterized by their spectral response and their current density versus voltage curves under AM 1.5 illumination of 100 mW cm^{-2}. The spectral response is expressed by the external quantum efficiency (IPCE) which is the ratio of the photocurrent to incoming photons flux: IPCE = 1240 $J_{ph}/\lambda I_0$, where J_{ph} is the photocurrent density (Acm^{-2}), I_0 is the light intensity (Wm^{-2}), and λ is the wavelength (nm) [17]. Figure 3 shows the spectral response of FTO/PEDOT:PSS/F8T2/C$_{60}$/Al devices for different active layer thickness: 18, 30, 40, and 60 nm. The external quantum efficiency spectra of the devices follow the absorption coefficient ($\alpha = 4\pi k/\lambda$) dependence on wavelength of F8T2 [5, 18] and C$_{60}$, reflecting the contribution of the polymer and the molecule to the photocurrent [19]. The light harvesting contribution of F8T2 can be observed in the wavelength range from 400 to 500 nm. The comparison of the action spectra for each thickness shows that the photoconversion efficiency is higher for the device with active layer of 30 nm: the maximum IPCE value is around 80% under monochromatic illumination of λ = 450 nm. Devices with thicker F8T2 layer presented maximum IPCE around 50%. It is well known that although thicker layers can absorb more light, the light intensity at the interface is smaller, thus the exciton dissociation in the F8T2/C$_{60}$ device [20, 21].

The electrical characteristics under illumination of AM1.5 radiation of 100 mWcm^{-2} are shown in Figure 4, and the photovoltaic parameters obtained from these curves are summarized in Table 1. The device performance dependence on F8T2 thickness corroborates with the external quantum efficiency results. The 30 nm F8T2 layer exhibits a short-circuit current (J_{sc}) of 4.79 mAcm^{-2}, V_{oc} of 0.91 V, a fill factor of 50% and of 2.1%. Bilayer devices based on F8T2/C$_{70}$ which were prepared by using trichlorobenzene as solvent and annealed at 100°C, displayed η = 1.2% as it was previously reported by Kekuda et al. [7]. Devices with F8T2 thickness of 60 nm presented poor photovoltaic performance. It is well known that devices based on thick active layers have the efficiency compromised by the transport due to higher resistance of the layer, as it can be clearly seen in Figure 4. In Figure 4 is also presented an equivalent circuit for photovoltaic device under illumination considered as a current source with a diode in parallel. We calculate the series resistance R_s of equivalent circuit associated with the solar cells by using the modified method for IEC 60891 following Kunz and
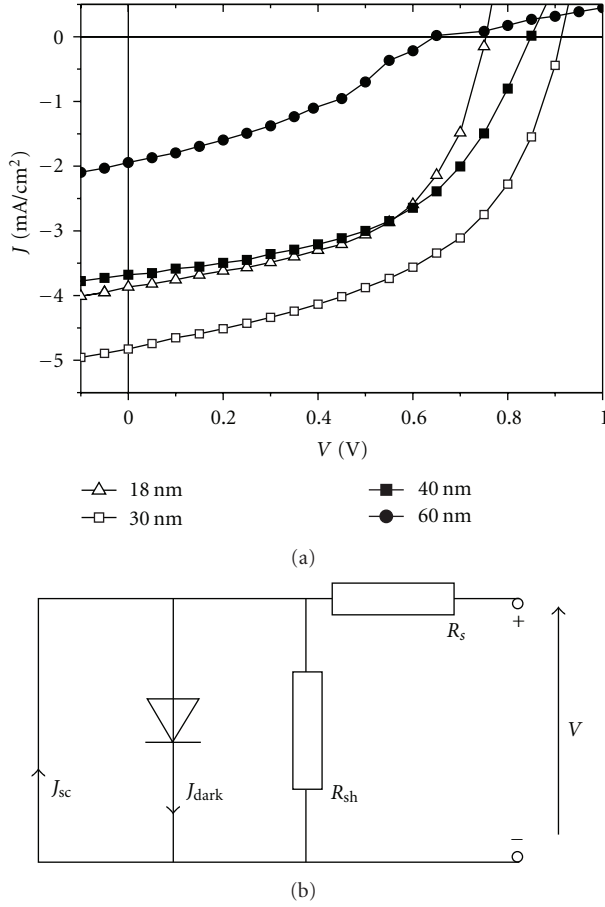
(a)

(b)

FIGURE 4: (J-V) curves under AM 1.5 illumination of 100 mWcm^{-2} for the FTO/PEDOT : PSS/F8T2/C$_{60}$/Al devices with different thickness of the F8T2 layer. An equivalent circuit simplified for a photovoltaic device, where R_s and R_{sh} are the series and shunt resistance, respectively.

Wagner [22]. Generally, the loss mechanisms in photovoltaic devices are divided in series resistance (R_s), which is related with the loss by charge carrier trapping or recombination of free charges, and shunt resistance (in parallel with the current source) (R_{sh}), which is related with leakage phenomena. R_s increases with the active layer thickness due to the increasing of the probability of a charge carrier to be trapped. In our devices, the series resistance increased with the F8T2 thickness for 30 nm the R_s was 77 Ω, for 40 nm the R_s was 198 Ω, and for 60 nm the R_s was 445 Ω. In the case of 18 nm the R_s was 150 Ω. This value did not follow the general behavior of resistance versus polymer thickness suggesting that the film formation indeed modifies the charge transport.

The electrical properties of these bilayer devices were also investigated by measuring the current versus voltage characteristics in dark. The study of forward current of bi-layer diodes is not so straight forward to do. F8T2 and C$_{60}$ have different electron affinities values in order to promote the exciton dissociation. The interface barrier of F8T2/C$_{60}$ is high enough to prevent the passage of charges through it, forming high charge density in each layer with a maximal recombination zone near the interface, resulting in a monop-
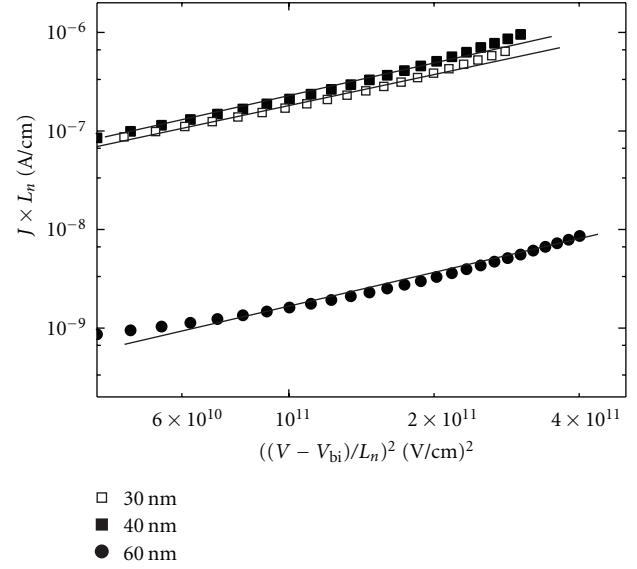

FIGURE 5: A log-log plot of the current density in dark times the C$_{60}$ thickness by the square of the voltage across the whole device divided by the C$_{60}$ thickness for three different values of the F8T2 thickness. All the linear fittings have angular coefficients equal to one, which characterize the Mott-Gurney law.

olar current density of hole inside the polymer layer and electrons inside the molecule layer [23]. Also, as the devices were fabricated with two different work functions electrodes ($\Phi_{PEDOT} \approx 5.2$ eV and $\Phi_{Al} \approx 4.2$ eV), a built-in potential (V_{bi}) is established in the organic layers at zero bias. Before attempting to model current versus field data [24], this inherent potential V_{bi} must be subtracted from the applied voltage. Based on earlier reports in literature, it was found that the built-in potential is equal to the open-circuit photovoltage (V_{oc}) of the device at low temperature [25]. In this work, the V_{oc} for each F8T2 thickness from Figure 2(b) is considered as the built-in potential value. Considering that, plotting the data from the current versus voltage curve in dark as a log-log plot of the $J \times L(C_{60})$ versus $((V - V_{bi})/L(C_{60}))^2$ (Figure 5), it is possible to notice that all the linear fittings have angular coefficient equal to one, which characterize the Mott-Gurney law of space charge limited current (SCLC) described by the expression [26]:

$$J = \frac{9}{8} \varepsilon_0 \varepsilon_r \mu \frac{(V - V_{bi})^2}{L^3}, \tag{1}$$

where $\varepsilon_0 \varepsilon_r$ is the permittivity of the polymer, μ the electron mobility, and L the thickness of the C$_{60}$ layer. The space charge limited current flowing in the device is induced by effective thickness-dependent mobilities of the charges in the respective layer of the device, spatial charge of holes in the polymer, and electrons in the molecule layers. The linear fittings of SCLC scaling plots for the fixed C$_{60}$ thickness show that in each material layer we have a simple Mott-Gurney law. Thus, the charge transport in these devices is a property of the interface polymer/C$_{60}$. From the different curves for different polymer thickness, it follows that the effective mobility of holes and electrons are dependent on the ratio

between the polymer and C_{60} layers' thickness. Despite the fact that a power conversion efficiency of 2.1% was achieved for one combination of thickness in these bi-layer devices, the analysis of the electrical properties in dark indicates that the mobility of charges in these devices still limits the efficiency.

4. Conclusion

We have investigated the effect of altering the F8T2 film thickness on the photovoltaic performance of devices based on the bilayer heterojunction with C_{60} molecules. It has been demonstrated that a power conversion efficiency of 2.1% can be achieved for F8T2 films with thickness equal to 30 nm and submitted to annealing at 100°C. From experimental and theoretical analyses, we have results that for such kind of systems the forward current is limited by spatial charge of holes in the polymer layer and electrons in the molecule layer. The series resistance calculated for an equivalent circuit of solar cells applied to our diodes plays an important part, depending not only on the layer thickness but also film morphology.

References

[1] I. Olle, Z. Fengling, and M. R. Andersson, "Alternating polyfluorenes collect solar light in polymer photovoltaics," *Accounts of Chemical Research*, vol. 42, no. 11, pp. 1731–1739, 2009.

[2] L. Akcelrud, "Electroluminescent polymers," *Progress in Polymer Science*, vol. 28, no. 6, pp. 875–962, 2003.

[3] B. Zhao, D. Liu, L. Peng et al., "Effect of oxadiazole side chains based on alternating fluorene-thiophene copolymers for photovoltaic cells," *European Polymer Journal*, vol. 45, no. 7, pp. 2079–2086, 2009.

[4] G. L. Schulz, X. Chen, and S. Holdcroft, "High band gap poly(9,9-dihexylfluorene-alt-bithiophene) blended with [6,6]-phenyl C_{61} butyric acid methyl ester for use in efficient photovoltaic devices," *Applied Physics Letters*, vol. 94, no. 2, Article ID 023302, 2009.

[5] J. H. Huang, C. Y. Yang, Z. Y. Ho et al., "Annealing effect of polymer bulk heterojunction solar cells based on polyfluorene and fullerene blend," *Organic Electronics: Physics, Materials, Applications*, vol. 10, no. 1, pp. 27–33, 2009.

[6] J. H. Huang, K. C. Li, D. Kekuda et al., "Efficient bilayer polymer solar cells possessing planar mixed-heterojunction structures," *Journal of Materials Chemistry*, vol. 20, no. 16, pp. 3295–3300, 2010.

[7] D. Kekuda, J. H. Huang, K. C. Ho, and C. W. Chu, "Modulation of donor-acceptor interface through thermal treatment for efficient bilayer organic solar cells," *Journal of Physical Chemistry C*, vol. 114, no. 6, pp. 2764–2768, 2010.

[8] A. G. Macedo, C. F. N. Marchiori, I. R. Grova, L. Akcelrud, M. Koehler, and L. S. Roman, "Hole mobility effect in the efficiency of bilayer heterojunction polymer/C_{60} photovoltaic cells," *Applied Physics Letters*, vol. 98, p. 253501, 2011.

[9] C. D. Canestraro, M. C. Schnitzler, A. J. G. Zarbin, M. G. E. da Luz, and L. S. Roman, "Carbon nanotubes based nanocomposites for photocurrent improvement," *Applied Surface Science*, vol. 252, no. 15, pp. 5575–5578, 2006.

[10] R. Valaski, C. D. Canestraro, L. Micaroni, R. M. Q. Mello, and L. S. Roman, "Organic photovoltaic devices based on polythi-ophene films electrodeposited on FTO substrates," *Solar Energy Materials and Solar Cells*, vol. 91, no. 8, pp. 684–688, 2007.

[11] A. C. Arias, L. S. Roman, T. Kugler, R. Toniolo, M. S. Meruvia, and I. A. Hümmelgen, "Use of tin oxide thin films as a transparent electrode in PPV based light-emitting diodes," *Thin Solid Films*, vol. 371, no. 1, pp. 201–206, 2000.

[12] H. Sirringhaus, M. Bird, T. Richards, and N. Zhao, "Charge transport physics of conjugated polymer field-effect transistors," *Advanced Materials*, vol. 22, no. 34, pp. 3893–3898, 2010.

[13] J. C. Hummelen, B. W. Knight, F. Lepeq, F. Wudl, J. Yao, and C. L. Wilkins, "Preparation and characterization of fulleroid and methanofullerene derivatives," *Journal of Organic Chemistry*, vol. 60, no. 3, pp. 532–538, 1995.

[14] S. A. Backer, K. Sivula, D. F. Kavulak, and J. M. J. Fréchet, "High efficiency organic photovoltaics incorporating a new family of soluble fullerene derivatives," *Chemistry of Materials*, vol. 19, no. 12, pp. 2927–2929, 2007.

[15] G. Zhao, Y. He, Z. Xu et al., "Effect of carbon chain length in the substituent of PCBM-like molecules on their photovoltaic properties," *Advanced Functional Materials*, vol. 20, no. 9, pp. 1480–1487, 2010.

[16] L. S. Roman, R. Valaski, C. D. Canestraro et al., "Optical band-edge absorption of oxide compound SnO_2," *Applied Surface Science*, vol. 252, no. 15, pp. 5361–5364, 2006.

[17] P. R. F. Barnes, A. Y. Anderson, S. E. Koops, J. R. Durrant, and B. C. O'Regan, "Electron injection efficiency and diffusion length in dye-sensitized solar cells derived from incident photon conversion efficiency measurements," *Journal of Physical Chemistry C*, vol. 113, no. 3, pp. 1126–1136, 2009.

[18] J. H. Huang, C. P. Lee, Z. Y. Ho, D. Kekuda, C. W. Chu, and K. C. Ho, "Enhanced spectral response in polymer bulk heterojunction solar cells by using active materials with complementary spectra," *Solar Energy Materials and Solar Cells*, vol. 94, no. 1, pp. 22–28, 2010.

[19] M. Koehler, L. S. Roman, O. Inganäs, and M. G. E. Da Luz, "Modeling bilayer polymer/fullerene photovoltaic devices," *Journal of Applied Physics*, vol. 96, no. 1, pp. 40–43, 2004.

[20] L. S. Roman, W. Mammo, L. A. A. Pettersson, M. R. Andersson, and O. Inganäs, "High quantum efficiency polythiophene/C_{60} photodiodes," *Advanced Materials*, vol. 10, no. 10, pp. 774–777, 1998.

[21] L. A. A. Pettersson, L. S. Roman, and O. Inganäs, "Modeling photocurrent action spectra of photovoltaic devices based on organic thin films," *Journal of Applied Physics*, vol. 86, no. 1, pp. 487–496, 1999.

[22] G. Kunz and A. Wagner, "Internal series resistance determinated of only one I-V curve under illumination," in *Proceedings of the 19th European Photovoltaic Solar Energy Conference*, p. 5BV.2.70, 2004.

[23] M. Koehler, L. S. Roman, O. Inganäs, and M. G. E. Da Luz, "Space-charge-limited bipolar currents in polymer/C_{60} diodes," *Journal of Applied Physics*, vol. 92, no. 9, pp. 5575–5577, 2002.

[24] G. G. Malliaras, J. R. Salem, P. J. Brock, and C. Scott, "Electrical characteristics and efficiency of single-layer organic light-emitting diodes," *Physical Review B*, vol. 58, no. 20, pp. R13411–R13414, 1998.

[25] G. G. Malliaras, J. R. Salem, P. J. Brock, and J. C. Scott, "Photovoltaic measurement of the built-in potential in organic light emitting diodes and photodiodes," *Journal of Applied Physics*, vol. 84, no. 3, pp. 1583–1587, 1998.

[26] P. N. Murgatroyd, "Theory of space-charge-limited current enhanced by Frenkel effect," *Journal of Physics D*, vol. 3, no. 2, article 308, pp. 151–156, 1970.